



Study and Characterization of a Two-Way Satellite Time and Frequency Transfer Link using Software-Defined Radio solutions to both code and carrier-phase signals

J. Achkar⁽¹⁾, Y-J. Huang⁽²⁾, M. Fujieda⁽³⁾, D. Piester⁽⁴⁾, E. Staliuniene⁽⁴⁾, B. Chupin⁽¹⁾ and F. Arias⁽⁵⁾

(1) LNE-SYRTE, Observatoire de Paris - Université PSL, CNRS, Sorbonne Université, PARIS, France

(2) Telecommunication Laboratories (TL), Chunghwa Telecom Co. Ltd, Taoyuan, Taiwan

(3) National Institute of Information and Communications Technology (NICT), Tokyo, Japan

(4) Physikalisch-Technische Bundesanstalt (PTB), Braunschweig, Germany

(5) SYRTE, Observatoire de Paris - Université PSL, CNRS, Sorbonne Université, LNE, PARIS, France

Abstract

This paper presents a complete study and characterization of a two-way satellite time and frequency transfer link between two remote earth stations equipped with analog modems and software-defined radio receivers driven by atomic clocks. Techniques based on code-phase and carrier-phase measurements were developed to compute time and frequency deviations between these clocks. A comparison of different methods using conventional bandwidth, broadband, carrier-phase information and software-defined radio solution is given. In addition, the paper is completed by a description of calibration aspects, more specifically on the software-defined radio link, an essential step in calculating the differences between remote time scales with very high accuracy, reaching a level of uncertainty of the order of 0.5 nanosecond.

1 Introduction

For more than 15 years, Two-Way Satellite Time and Frequency Transfer (TWSTFT) has been a major technique [1] operated continuously and regularly in about 20 timing laboratories worldwide. Processed data are used for the generation of Coordinated Universal Time (UTC). The technique relies on a protocol for transmitting and receiving clock signals via a telecommunication satellite using carrier frequencies in the Ku band. For this purpose, Satellite Time and Ranging Equipment (SATRE) modems, developed and marketed by TimeTech GmbH, are being operated in the earth stations of the contributing laboratories. The precision of TWSTFT as observed today (with its financial restrictions on the lease of satellite transponder bandwidth) is limited by an apparent daily variation pattern (diurnal) in the TWSTFT results. In consequence, calibrations using a mobile TWSTFT station are usually limited by the same effect. Recent developments of Software-Defined Radio (SDR) receivers for TWSTFT have demonstrated superior performance in terms of stability [2, 3], and thus the BIPM processes the SDR measurements of the TWSTFT link between OP (LNE-SYRTE) and PTB as a UTC backup link since the end of 2017. However, the accuracy in time remained limited because the SDR TWSTFT link was calibrated by alignment with the corresponding SATRE TWSTFT link.

More recently, the first calibration of the SDR TWSTFT link between OP and PTB using a travelling SDR receiver developed in OP driven by a calibration software developed by OP in collaboration with TL was performed [4]. This work is aimed to improve the calibration accuracy and thus the uncertainty of operational time links, e.g. to improve the generation of UTC and the Galileo ground segment timing infrastructure. Since February 2020, this link has been used as the first SDR link by the BIPM for the calculation of UTC.

2 Code-phase TWSTFT Technique

Code-phase TWSTFT is based on the exchange of timing signals through telecommunication satellites. It is done by transmission and reception of Radio Frequency (RF) signals, containing Binary Phase-Shift Keying (BPSK) modulated Pseudo-Random Noise (PRN) codes on the Intermediate Frequency (IF) by a modem. The phase modulation is synchronized with the local clock, and the modem generates a one-pulse-per-second (1 pps) output, synchronous with the BPSK sequence. Each station uses a dedicated PRN code for its BPSK sequence in the transmitted signal. The receiving equipment generates the BPSK sequence of the remote station and reconstitutes a 1 pps tick from the received signal. The difference between the two 1 pps signals (TW) is measured by a time-interval counter. Following a pre-arranged schedule, a pair of stations lock on the code of the corresponding remote station for a specified period, measure the signal's time of arrival, and store the results. After exchanging the data records, the difference between the two clocks, e.g. $UTC(1)$ and $UTC(2)$, can be computed according to eq. (1) considering the $UTC(k)$ s reference delays ($Refdelay$):

$$\begin{aligned}
 UTC(1) - UTC(2) &= 0.5 \cdot [TW(1) - TW(2)] \\
 &+ 0.5 \cdot \{[SPU(1) - SPD(1)] - [SPU(2) - SPD(2)]\} \\
 &+ 0.5 \cdot \{[SCU(1) - SCD(1)] - [SCU(2) - SCD(2)]\} \\
 &\quad + 0.5 \cdot [SPT(1) - SPT(2)] \\
 &+ 0.5 \cdot \{[Tx(1) - Rx(1)] - [Tx(2) - Rx(2)]\} \\
 &\quad + [Refdelay(1) - Refdelay(2)]
 \end{aligned} \tag{1}$$

The delays along the signal paths (SPT , SPU , SPD) cancel due to reciprocity to first order. The equipment delays (Tx , Rx) and delays due to the Sagnac effect (SCU , SCD) are constant to first order and can be determined (see [1] for

further details). The accuracy of the result then depends on the residual effects and uncertainties.

3 Carrier-phase TWSTFT Technique

The Carrier-phase method is also based on the exchange of clock signals through geostationary satellites generated by a set of two remote earth stations, but in a more complex scheme [5, 6]. Four sets of phase information are required to determine the intrinsic characteristics of the Carrier-Phase TWSTFT (CP-TWSTFT) system: the time difference between the two remote clocks, the fluctuations of the phase induced by the signal translation in the satellite, and the two distances between the satellite and the two earth stations involved. To do so, each station receives two types of signals through the satellite, the two-way signal emitted by the remote station and its own ranging signal. The transmitted signal is shifted because of the Doppler Effect due to the slight motion of the geostationary satellite and the satellite local oscillator frequency. The phase information Φ of the signal includes the ionospheric $I(t)$ and tropospheric delays along the signal path multiplied by the signal angular frequency ω including the Doppler shift. Usually, the distance from one station to the satellite and the corresponding distance from the other station to the satellite are not symmetrical. As a result, there is a difference in the arrival times of signals from the two stations at the satellite. It is assumed that the residual error on the frequency translation on board the satellite is stable during this time difference. As in TWSTFT, the tropospheric delays are cancelled. However, the ionospheric correction term is not negligible and must be calculated and taken into account in CP-TWSTFT. From the above considerations, the time difference between the two earth stations can be computed according to eq. (2):

$$\begin{aligned} \tau_1(t) - \tau_2(t) = & \left(\frac{\omega_u + \omega_d}{4 \omega_u \omega_d} \right) [\Phi_{1-2}(t) - \Phi_{2-1}(t)] \\ & - \left(\frac{\omega_u - \omega_d}{4 \omega_u \omega_d} \right) \cdot [\Phi_{1-1}(t) - \Phi_{2-2}(t)] \quad (2) \\ & + 0.5 \cdot \{ [I_d^1(t) - I_u^1(t)] - [I_d^2(t) - I_u^2(t)] \} \end{aligned}$$

4 Setting-up the code-phase SDR-TWSTFT experiment

A SDR receiver can be operated in parallel with a SATRE modem, and data generated that way are free from the effects of processing in the SATRE receive part. In each station the transmission signal is generated by the SATRE modem and the down-converted received signal is split and fed to both the SDR setup and SATRE modem. The key components of the SDR consist of an Analog to Digital (A/D) sampler recording the received PRN signal at the 70 MHz IF, and a Graphic Processing Unit (GPU) card installed in a computer for processing the TWSTFT measurements with dedicated software developed by TL. In addition, one or two amplifiers and a bandpass filter are used to optimize the input signal to the A/D sampler. The arrival time of the signal is thus determined, by SATRE

modem and SDR receiver independently, as illustrated in Figure 1.

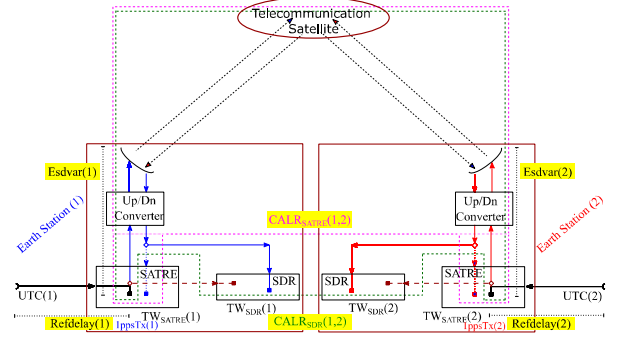


Figure 1. Illustration of the main signal paths of a TWSTFT link based on the combination of SATRE modems with SDR receivers to compare UTC(k)s.

5 Setting-up the carrier-phase TWSTFT experiment

The CP-TWSTFT experiment was performed using a microwave link between PTB and OP through the ASTRA 3B satellite located at orbital position of 23.5° East. At the same time, the Ku band transponder was allocated in the frame of the EURAMET research project ITOC [7], for which the cost was shared equally between the four metrology institutes NPL, INRIM, PTB and OP. The CP-TWSTFT platform was developed and provided by NICT. In order to avoid interferences with the broadband two-way code signals of the ITOC experiment (20 MChip/s), the CP-TWSTFT technique used a narrow frequency band with a bandwidth of 200 kHz far from the frequency center of the allocated bandwidth on the transponder. A PRN code of 127.75 kChip/s is generated by an arbitrary waveform generator whose output bandwidth was limited by a 200 kHz digital filter. The IF signal with an offset frequency, up-converted to an RF signal, then amplified by a solid-state power amplifier and fed to the antenna. The RF signal received by the antenna is amplified by a low-noise amplifier (LNA) and down-converted to an IF signal, then filtered through an active band-pass filter of 2 MHz. In the last process, the signal is sent to an A/D sampler and then analyzed by software. In contrast to the configuration adopted in PTB where a separate station for CP-TWSTFT was used, the OP station (OP02) was shared by the broadband TWSTFT and CP-TWSTFT measurements, as shown in Figure 2.

Both measurements were performed simultaneously. The received signal was split into two components after the output port of the LNA, and the two components were input into different frequency down-converters. However, a degradation in the measurement precision caused by the combined processing of the two signals was observed.

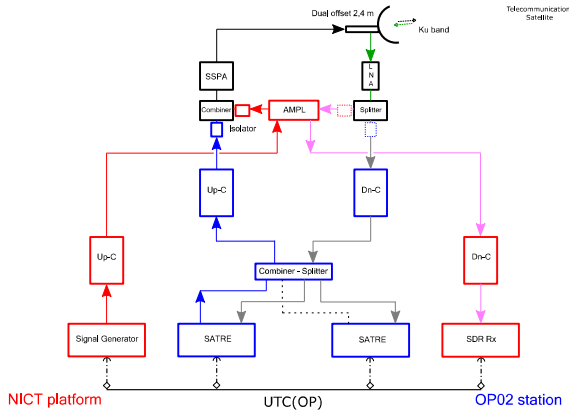


Figure 2. CP-TWSTFT setup in OP02 earth station equipped with SATRE modems and NICT platform.

6 Link characterization by multi-techniques

A set of results characterizing a single link for comparing remote atomic clocks presented in this section grouping together measurements obtained at different periods using different techniques based on two-way microwave links via telecommunication satellites. Figure 3 and Figure 4 show the performance of the OP-PTB two-way link using the conventional technique, broadband and carrier phase information. Time difference data of the latter techniques are taken and reproduced from [7] and [6], respectively.

The carrier-phase results are comparable to those provided by the broadband TWSTFT measurement and about one order of magnitude better than those given by the conventional TWSTFT technique. Besides other investigations, the effect of the used power splitter-combiner must be further studied (see Fig. 2) to achieve microwave link frequency instability below 10^{-16} level. Figure 5 and Figure 6 show the performance of the OP-PTB two-way links using the software-defined radio solution, calculated on data recorded over a long period.

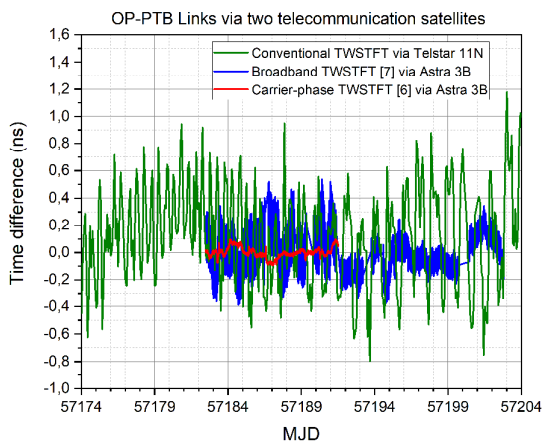


Figure 3. Time difference of the various TWSTFT link techniques (20 MChip/s code-phase data in blue collected continuously every second, 1 MChip/s code-phase data in green performed for 2 min every 2 h, carrier-phase data in red recorded continuously every second) between OP and

PTB. For the carrier-phase link, the time difference is fluctuating within 200 ps after removing a linear fit.

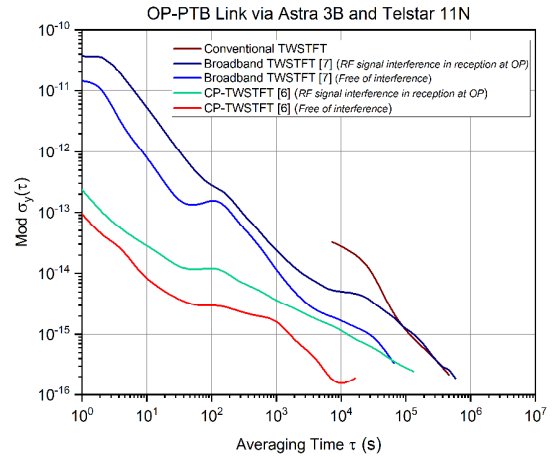


Figure 4. Modified Allan deviation for all TWSTFT link data between OP and PTB, calculated over available measurement periods, not only limited to the data and period presented in Fig.3. For the carrier-phase link, a frequency instability of 4×10^{-16} is reached at an averaging time of 1 d.

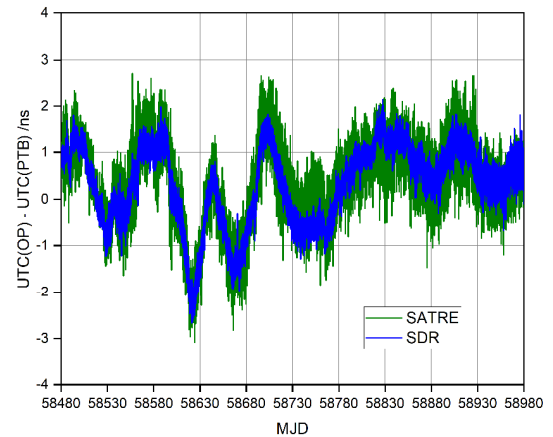


Figure 5. Time scales difference between OP and PTB by SATRE and SDR TWSTFT links.

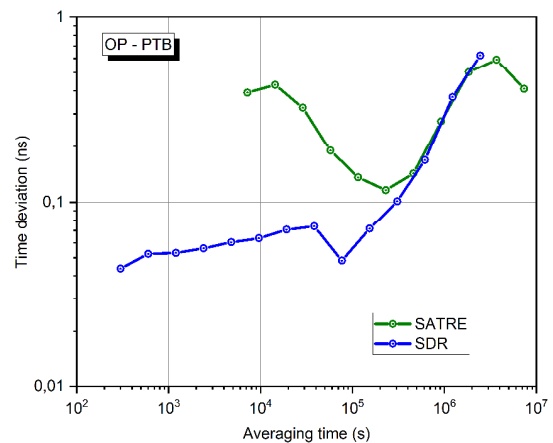


Figure 6. Time deviation for the OP-PTB link calculated from the data plotted in Fig. 5. For averaging times below

1-day, the time instability of the SDR link remains below 100 ps. Above 1-day, the time deviations are dominated by the clocks fluctuations.

From the figures above, the improvement brought by the SDR solution is obvious with in particular a significant reduction of the short-term instability.

7 Calibration of the OP-PTB SDR TWSTFT link

The calibration exercise carried out in 2019 [4] for the first time, with a calibration kit based on a travelling SDR receiver (Figure 7) accompanying a TWSTFT portable earth station equipped with a SATRE modem showed a significant reduction in the calibration uncertainty (Figure 8) estimated at 0.5 ns which corresponds to an expanded uncertainty of 1 ns ($k = 2$) necessary to improve UTC and thus its prediction. The lessons learned are to: i) consider where possible, 1ppsTx as the best Common Reference Point (CRP) for calibration purposes, ii) use only one single counter, which travels with the mobile station throughout the calibration campaign. The associated uncertainty component is thus reduced. Another major advantage of systematically measuring the reference delay parameter, during a calibration process, is to ensure that a CRP has been applied to both the fixed station as a DUT, and to the mobile station connected in common clock mode. Thus, a bias can be clearly ruled out.

Areas for improvement of satellite clock comparison techniques should focus on complete software-defined radio solutions (SDR transmission and reception, digital modems), implementation of standard microwave satellite simulator and consideration of increasing frequency satellite link to the Ka band.

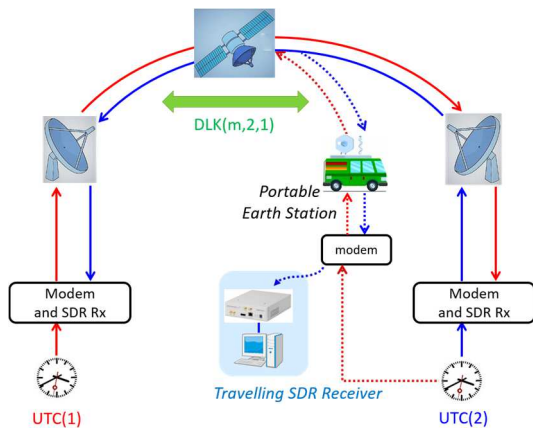


Figure 7. Calibration process in a link-mode configuration involving two fixed stations and a mobile station, all equipped with SATRE modems and SDR receivers.

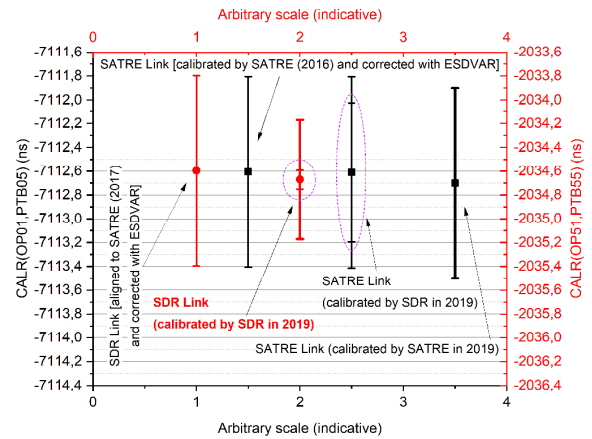


Figure 8. SDR and SATRE TWSTFT OP-PTB links calibration results performed in 2019 using a travelling SDR receiver [4]. Comparison with calibration (SATRE) and alignment (SDR) results achieved in 2016 [8], 2017 [2] and 2019 [9], and corrected with ESDVAR values; the respective error bars represent the combined uncertainties resulted from calibration or alignment. For 2019 values calibrated by SDR, two types of error bars are shown: large error bars represent the combined uncertainties while the reduced error bars represent the standard deviation on the mean of the calculated values by considering different calibration configurations (site mode, link modes and two-link mode).

8 Acknowledgements

The authors thank the CCTF WG on TWSTFT for their support, Andreas Bauch (PTB), Victor Zhang (NIST) and Héctor Esteban (ROA) for their contributions.

9 References

1. "The operational use of two-way satellite time and frequency transfer employing pseudorandom noise codes", *Recommendation ITU-R TF.1153-4*, Geneva 2015. <https://www.itu.int/rec/R-REC-TF.1153/en>.
2. Z. Jiang et al., "Use of software-defined radio receivers in two-way satellite time and frequency transfers for UTC computation", *Metrologia*, **55**, pp. 685-698, 2018.
3. Z. Jiang et al., "Improving Two-Way Satellite Time and Frequency Transfer with Redundant Links for UTC Generation", *Metrologia*, **56**, 2, <https://doi:10.1088/1681-7575/aafced>, 2019.
4. J. Achkar et al., "First Calibration of the UTC TWSTFT Link between OP and PTB Using a Travelling SDR Receiver", *Calibration report*, BIPM No. 0517-2020.
5. M. Fujieda et al., "Carrier-phase two-way satellite frequency transfer over a very long base-line", *Metrologia*, **51**, 2014.
6. J. Achkar et al., "Study of the OP-PTB Link by Carrier-Phase Two-Way Satellite Time and Frequency Transfer", *Conference on Precision Electromagnetic Measurement*, July 2016.
7. F. Riedel et al., "Direct comparisons of European primary and secondary frequency standards via satellite techniques", *Metrologia*, **57**, doi.org/10.1088/1681-7575/ab6745, 2020.
8. F.J. Galindo et al., "European TWSTFT calibration campaign 2016", *Calibration Report*, BIPM No. 0437-2016.
9. H Esteban, "TWSTFT Calibration Report", GAL-TN-ROA-GSOP-20191001 v3, BIPM No. 0503-2019.